

Stability of Geomembrane Surface Barrier of Earth Dam Considering Strain-softening Characteristic of Geosynthetic Interface

Haimin Wu* and Yiming Shu**

Received January 23, 2011/Revised 1st: June 15, 2011, 2nd: August 7, 2011, 3rd: November 1, 2011/Accepted January 8, 2012

Abstract

Geosynthetic interfaces are characterized by strain-softening behaviors that exhibit a reduction in shear stress at relative shear displacements beyond peak strengths. The traditional practice in assessing the stability of geosynthetic barrier systems is based on Limit Equilibrium Method (LEM) which cannot consider the strain-softening behavior of interfaces. The safety factors calculated by LEM may overestimate the stability of geosynthetic barrier systems. A method combining LEM with numerical analysis for evaluating stability of geomembrane surface barrier of earth dam was proposed in this paper. The formula of calculating the factor of safety for geomembrane barrier systems taking account of the effect of interface strain-softening was derived. An example of composite geomembrane lined earth dam was numerically analyzed to verify the developed method. The calculated factor of safety is between the results that calculated from LEM using peak shear strength and residual shear strength. Through comparatively analysis with LEM results, it is suggested to use peak shear strengths along the basal interface and residual shear strength along the side slope interface in evaluating stability of geomembrane surface barrier of earth dam using LEM.

Keywords: *geosynthetic barrier systems, strain-softening of interface, stability, limit equilibrium method, numerical analysis*

1 Introduction

Due to the numerous advantages over traditional barrier materials in cost, imperviousness, construction, and practical considerations, geomembranes are increasingly used as waterproofing layer in earth and rock dam. A general cross section of geomembrane surfaced lined earth dam is shown in Fig. 1, geomembrane barrier systems are commonly comprised by three layers, namely basal support layer, geomembrane barrier and protection cover layer. In Chinese design specification for rolled earth-rock fill dam, the geomembrane barrier is usually used with composite geomembrane compounded by two layer of non-woven geotextiles and a layer of HDPE or PVC geomembrane. The composite geomembrane is glued on the surface of the support layer. For high earth dam, a wedge-shaped protection cover is usually used to increase the stability of the barrier systems (Ministry of Water Resources of the People's Republic of China, 1998). Due to low shear strength, the interface between composite geomembrane and protection cover soil often become the preferential failure surface. So the stability of wedge-shaped protection cover is a critical problem for the design of geomembrane surface barrier of earth dam. For example, Giroud *et al.* (1990) reported a slip failure of protection cover along the interface between geotextile and geomembrane in an embankment. Through investigation

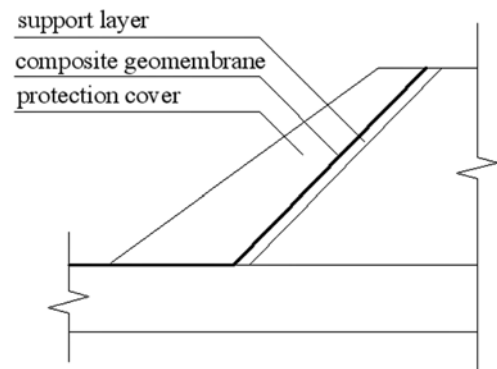


Fig. 1. Geomembrane Barrier of Earth Dam

and analysis, they found that it was the overestimation of interface shear strength and dynamic stresses resulting from the trafficking of vehicles had caused the incident.

The stability assessment of geomembrane barrier is of major importance for the design of such barrier systems. Many researchers have worked on this subject. From the literature it can be seen that the researches mainly focus on two aspects. The first is about the shear strength properties and parameters of geosynthetic interface. The other is about the analysis methods of the stability of geosynthetic barrier systems on slope.

*Ph.D., College of Water Conservancy and Hydropower Engineering, Hohai University, Nanjing 210098, P. R. China (Corresponding Author, E-mail: haimin-wu@hotmail.com)

**Professor, College of Water Conservancy and Hydropower Engineering, Hohai University, Nanjing 210098, P. R. China (E-mail: shym@hhu.edu.cn)

The geosynthetic interface shear strength is an important factor for the stability of geosynthetic barrier along slope. The resistance to the failure of geosynthetic barrier system (as Fig. 1) is mainly provided by the shear strengths of geosynthetic-soil interface on the slope and base. So obtaining the appropriate interface shear strength parameters is the basis of assessing the stability of the geosynthetic barrier. The common practice of obtaining the parameters of interface strength is to carry out a number of site-specific or laboratory tests. Dixon *et al.* (2002) proposed some guidance on obtaining characteristic values of geosynthetic interface shear strength parameters through a limited number of tests for use in design calculations. However, Dixon *et al.* (2006) indicated that common practice of obtaining the geosynthetic interface strength parameters cannot provide sufficient information on the variability of interface strength for design. They proposed a summary of measured strengths and an assessment of variability. Through reliability analyses they found that relatively high probabilities of failure are obtained when using variability values from the literature and an internal database. The use of repeatability data produces lower probabilities for typically used factors of safety, although they are still higher than recommended target probability of failure values. Sia and Dixon (2007) found that normal distribution is suitable to represent interface shear strengths and their derived strength parameters especially when variability is small. Through calculation and comparison, they concluded that variability and uncertainty computed using global and inter-laboratory datasets yield overly conservative outcomes when adopted in design.

Through large displacement shear box tests, it has been reported by several authors, e.g., Seed *et al.* (1988), Byrne (1994), Shallenberger and Filz (1996), Jones and Dixon (1998) and Gomez and Filz (1999) that most geosynthetic interfaces are susceptible to strain softening behaviors. That means the peak strength is significantly greater than the residual strength for geosynthetic interfaces. The shear stress-displacements relationship exhibits a reduction in shear stress beyond peak shear strengths. Then subsequent shear displacements result in a further decrease in shear stress to a constant or residual value. When calculating the factor of safety with the LEM, the value of shear strength must be selected from either peak strength, residual strength or factored values. In actual working condition, deformations of barriers of dam or landfill resulted from the water pressure or waste settlements may induce large shear displacement at the geosynthetic interfaces. Under condition of large deformations, the mobilized shear strengths will vary along the entire interface on the basal and slope. So the actual distribution of the mobilized shear strengths of the failure surface should be taken into account in analyzing the stability of geosynthetic barrier systems.

The analysis methods of the stability of geosynthetic barrier systems had been of great interest in the past decades. The earliest used method is Limit Equilibrium Method (LEM) proposed by Giroud and Beech (1989) and Koerner *et al.* (1991). In analysis with LEM, the cover of barrier systems is divided into two wedges. And it is assumed that the two parts reach limit

equilibrium states at the same time. The factor of safety can be obtained by solving a quadratic equation of one variable. This method has been used extensively in design of geosynthetic barrier systems. The second method is the limit method which was proposed by Koerner (1994). This method can calculate the tensile forces in each layer of the barrier system. But due to ignoring the shear resistances provided by cover soil buttress and waste buttress, the tensile force in each structural component will be overestimated. The two methods are both on basis of limit equilibrium concept. Their main issues are that they are unable to consider the effect of the deformation of different materials and the interaction between them.

In order to consider the deformation of different structural components within the barrier system, several methods were proposed, such as, displacement compatibility method and strain compatibility method (Long *et al.*, 1994), numerical analysis method (Villard *et al.*, 1999; Filz *et al.*, 2001) and the method can assess both the local failure and integrity of the barrier system (Jones and Dixon, 2005).

The most important improvement of the method proposed by Long *et al.* (1994) is that it can consider both force equilibrium and displacement compatibility. With this method, more accurate tensile forces within each structural component of the barrier system can be predicted than the results from the limit method.

The numerical method developed in recent years can be used to model the strain softening behavior of geosynthetic interface. Through numerical analyzing of the entire barrier systems, the distributions of the relative shear displacement and mobilized shear strength along geosynthetic interfaces can be obtained. Villard *et al.* (1999) used finite element method to model the different components and their interaction of geosynthetic barrier systems in response to the filling process of granular drainage materials. Through comparing with a full-scale experiment, the calculated results presented a satisfactory agreement with the observed results. Filz *et al.* (2001) used the finite element method to analyze the progressive failure process along geosynthetic interfaces induced by gradual filling of the landfill. The results from numerical analyses indicated that progressive failure is likely to have a significant effect on the stability of Municipal Solid Waste (MSW) landfills. They concluded that the designer should consider the strain softening behavior of geosynthetic interfaces of landfill lining systems.

Jones *et al.* (2005) presented a method which can assess both the lining stability and integrity of geosynthetic barrier systems. Through modeling the strain-softening behaviors of geosynthetic interfaces, the local failure of barrier systems can be assessed. They also compared the use of limit equilibrium and numerical analysis techniques for assessing stability of a lining system containing a strain softening interface. Their results demonstrated that waste settlement can result in slippage of lining components on the side slope even though the global stability factor of safety is adequate. They suggested that traditional limit equilibrium techniques cannot be used to assess local failure of geosynthetic lining systems. From Jones' study, it can be indicated that: (1)

the numerical analysis method can model the interactions and strain softening behaviors of geosynthetic interfaces included in geosynthetic lining systems of landfill; (2) without considering the effect of strain softening behaviors of geosynthetic interfaces, the limit equilibrium method may overestimate the factor of safety for geosynthetic lining systems along slope.

The studies presented above are mainly concentrated on the stability and performance of geosynthetic lining systems of landfill. But the research on the stability of geosynthetic barrier of earth dam had been rarely reported. Wu *et al.* (2008) made an investigation on failure of a geosynthetic lined reservoir. On basis of observation in the field and interface strength testing by large direct shear tests and large tilt table tests, the author analyzed the stability and deformation of the geomembrane by analytical and numerical methods, respectively. The results indicated that a poor initial design and choice of non-textured geomembrane are the main reason of failure. However, their study didn't take account for the effect of strain softening behavior of geomembrane interface and the deformation of dam.

In this study, a formula of calculating the factor of safety for geomembrane barrier taking account of the effect of interface strain-softening is derived. The nonlinear strain softening interface model is incorporated into FLAC^{3D} to simulate the geomembrane-soil interaction. The method of evaluating stability of geomembrane barrier of earth dam combining limit equilibrium and numerical analysis methods was presented. An example of composite geomembrane lined earth dam is numerically analyzed to verify the developed method. The calculated factor of safety calculated by the developed method is compared with the results of LEM using three types of interface shear strength, namely, peak shear strength in the entire interface, residual shear strength in the entire interface, peak shear strength on the slope and residual shear strength at the base, respectively.

2. Calculation Principles

2.1 Traditional LEM

Due to reasonable principle and less computation work, the LEM proposed by Koerner *et al.*, 1991) has been used extensively in China and abroad. The typical geomembrane surface barrier of earth dam is shown in Fig. 2. The field case was idealized as two dimensional and a plane-strain analysis was performed by considering a slice of embankment with a thickness of 1 m. The barrier is divided into an active wedge (A) and a passive wedge (P). The two wedges are assumed to reach limit failure state at the same time. The wedge-shaped protection cover is made of coarse grains which is capable of draining the water in the barrier. The procedure for analysis of the stability is presented as follows.

For active wedge A:

$$E_A \cdot \sin\left(\frac{\alpha + \omega}{2}\right) + T_A \cdot \sin \alpha + N_A \cdot \cos \alpha - W_A = 0 \quad (1)$$

$$N_A = W_A \cdot \cos \alpha \quad (2)$$

where W_A is total weight of the active wedge; N_A is effective

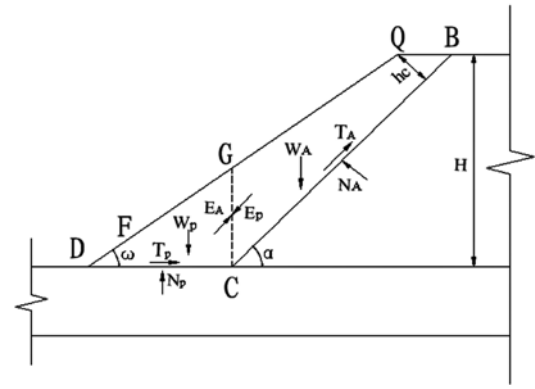


Fig. 2. Model for Stability Analysis

force normal to the failure plane of active wedge; T_A is shear resistance on the failure plane of active wedge; E_A is the inter-wedge force acting on the active wedge from passive wedge.

For passive wedge P:

$$T_P - E_P \cdot \cos\left(\frac{\alpha + \omega}{2}\right) = 0 \quad (3)$$

$$N_P = W_P + E_P \cdot \sin\left(\frac{\alpha + \omega}{2}\right) \quad (4)$$

where W_P is total weight of the passive wedge; N_P is effective force normal to the failure plane of passive wedge; T_P is shear resistance on the failure plane of passive wedge; E_P is the inter-wedge force acting on the passive wedge from active wedge.

The two inter-wedge forces E_P and E_P are equal in magnitude, but opposite in direction. The follow equation can be established:

$$E_A = E_P \quad (5)$$

The shear resistance on the failure plane of two wedges can be calculated by Mohr-Coulomb criteria:

$$T_A = \frac{N_A \cdot \tan \varphi + c_a \cdot l_1}{F_s} \quad (6)$$

$$T_P = \frac{N_P \cdot \tan \varphi + c_a \cdot l_2}{F_s} \quad (7)$$

where φ is interface friction angle between cover soil and geomembrane; c_a is interface apparent adhesion intercept between cover soil and geomembrane; l_1 is length of the failure plane of active wedge; l_2 is length of the failure plane of passive wedge; F_s is the factor of safety for the entire barrier based on LEM.

By combining the seven equations above, a quadratic equation of F_s can be established as follows:

$$a(F_s)^2 + b(F_s) + c = 0 \quad (8)$$

Where

$$a = (W_A - N_A \cdot \cos \alpha) \cos\left(\frac{\alpha + \omega}{2}\right);$$

$$c = (N_A \cdot \tan \delta + c_a \cdot l_1) \cdot \sin \alpha \cdot \sin\left(\frac{\alpha + \omega}{2}\right) \cdot \tan \delta;$$

$$b = -(W_A - N_A \cdot \cos \alpha) \cdot \sin\left(\frac{\alpha + \omega}{2}\right) \cdot \tan \delta - (N_A \cdot \tan \delta + c_a \cdot l_1)$$

$$\cdot \sin \alpha \cdot \cos \left(\frac{\alpha + \omega}{2} \right) - (W_p \cdot \tan \delta + c_a \cdot l_2) \cdot \sin \left(\frac{\alpha + \omega}{2} \right)$$

The formula of calculating the factor of safety can be solved as Eq. (9):

$$F.S = \frac{-b + \sqrt{b^2 - 4ac}}{2a} \quad (9)$$

So for a geomembrane surface barrier with given geometry and size, the factor of safety can be calculated by Eq. (9) based on the concept of limit equilibrium state.

2.2 Nonlinear Strain Softening Model of Geosynthetic Interface

As shown in Fig. 3, the typical relationship between shear stress and displacement of textured geomembrane/geotextile interface is derived from testing carried out using a 300 mm direct shear apparatus as described by Jones and Dixon (1998) according to the standard of BS 6906, Method of test for Geotextiles, Part 8 Determination of sand-geotextile frictional behavior by direct shear test. It can be seen that the nonlinear strain-softening property of geosynthetic interfaces exhibit a reduction in shear stress at displacements beyond peak strengths. The curve of shear stress vs. displacement can be divided as three stages: pre-peak stage, softening stage and residual stage. In the pre-peak stage, the shear stress increases from the origin with increasing displacement and show a nonlinear property until a peak value is achieved. In the softening stage, subsequent shear displacement results in a reduction in shear stress to a constant or residual value. In the residual stage, the shear stress keeps constant with the continuously increasing of shear displacement. Based on the results of interface tests conducted by Jones and Dixon (1998), a new interface constitutive model which combines the nonlinear hyperbolic model (Clough and Duncan, 1970) with displacement-softening model (Seo *et al.*, 2004) is employed to describe the nonlinear and strain-softening property of geosynthetic interface. The detailed constitutive relations of the new interface model will be introduced in subsequent section.

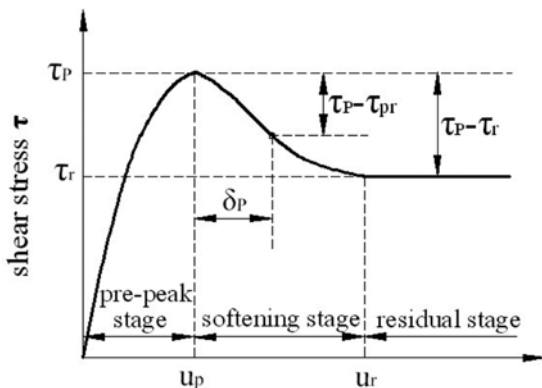


Fig. 3. Relationship between Shear Stress and Displacement of Geomembrane Interface

2.2.1 Pre-peak Stage

As shown in Fig. 3, pre-peak relationship between interface shear stress and displacement show a hyperbolic shape. So the pre-peak interface behavior can be represented by the nonlinear hyperbolic model (Clough and Duncan, 1970). The shear stiffness of interface can be expressed as:

$$K_s = K \cdot Pa \cdot \left(\frac{\sigma_n}{Pa} \right)^n \cdot \left[1 - R_f \frac{\tau}{c_p + \sigma_n \cdot \tan \phi_p} \right]^2 \quad (10)$$

where τ is the shear stress in nonlinear stage; ϕ_p is the peak friction angle of the interface; c_p is the peak cohesion of the interface; σ_n is the normal stress of the interface; Pa is atmospheric pressure; and K , R_f and n is the nonlinear parameters which can be derived from interface direct shear tests.

2.2.2 Softening Stage

In the softening stage, the shear stresses show a sharply reduction with the subsequent shear displacement. Post-peak shear strength reduction ($\tau_p - \tau_{pr}$) is normalized by the shear strength reduction from peak to residual value ($\tau_p - \tau_r$), represented by strength residual factor R (Skempton, 1964):

$$R = \frac{\tau_p - \tau_{pr}}{\tau_p - \tau_r} \quad (11)$$

where τ_{pr} is the post-peak shear strength; τ_p is the peak shear strength; τ_r is the residual shear strength; τ_p and τ_r can be calculated by Mohr-Coulomb criteria as following relations:

$$\tau_p = \sigma_n \cdot \tan \phi_p + c_p \quad (12)$$

$$\tau_r = \sigma_n \cdot \tan \phi_r + c_r \quad (13)$$

where ϕ_r is the residual friction angle of the interface; and c_r is the residual cohesion of the interface.

Through experimental observation of study on interface, Anubhav (2010) found the relationship between plastic shear displacement and residual factor (normalized shear strength degradation) follows “S”-shaped curve which can be effectively represented by following equation:

$$R = 1 - \exp(-A \cdot \delta_p^z) \quad (14)$$

Where δ_p is plastic shear displacement which is defined in Fig. 3; A and z are model parameters which can be obtained by nonlinear regression analysis from experimental data.

2.2.3 Residual Stage

After falling into residual stage, the shear stress reaches a stable state as the continuously increasing of shear displacement as shown in Fig. 3. The shear stress keeps a constant of residual shear strength. That can be calculated by following equation:

$$\tau = \tau_r \quad (15)$$

2.3 Mobilized Shear Resistance of Geomembrane Interface

In accessing the stability of geomembrane barrier with LEM, the resistance force of the entire barrier is provided by the shear

strength of the geomembrane-soil interface. While calculating the shear resistance of the two wedges by Eq. (6) and Eq. (7), it is assumed that the shear strengths along the interface are fully mobilized. In fact, the degree of mobilization will depend on the relative shear displacement along the interface due to the deformations of dam and the barrier systems. So the traditional method of calculating the factor of safety will lead to a large deviation from the results calculated using actual distribution of the mobilized shear strengths along the interface.

In order to get the distribution of mobilized shear strengths along the geomembrane interface due to the deformations of dam and the barrier systems, the strain softening relationship between shear stress and displacement of interface is taken into account. It is supposed that the geomembrane-soil interface on the slope is divided into m elements. The shear resistance force of the i^{th} interface element can be expressed by following equation:

$$T_i = \frac{f(\sigma_{ni}, u_i)}{F' \cdot S} \quad (16)$$

where the subscript i designates the order of the m interface elements; $f(\sigma_{ni}, u_i)$ is shear strength which is function of σ_{ni} and u_i of the i^{th} interface element; σ_{ni} is the normal effective stress of the i^{th} interface element; u_i is the relative shear displacement of the i^{th} interface element; $F' \cdot S$ is the factor of safety of the entire barrier considering the interface strain softening property.

Through numerical analysis of the geomembrane barrier of earth dam considering interface strain softening behavior, the distribution of mobilized shear stresses along the geomembrane interface can be obtained. The stresses states of any element along the interface can be divided into three types, namely, pre-peak state, softening state and residual state, which are in correspondence with the three stages of interface shear stress-displacement relationship shown in Fig. 3. Then according to the stress state the i^{th} interface element, the shear strength of this element can be calculated by the relations of the corresponding stage of interface shear stress-displacement relationship. So the mobilized shear strength of the i^{th} interface element can be expressed as follows:

$$f(\sigma_{ni}, u_i) = \begin{cases} \tau_{ip}, & u_i \leq u_{ip} \\ \tau_{ir}, & u_i > u_{ip} \end{cases} \quad (17)$$

where τ_{ip} and τ_{ir} are the peak and residual shear strength of the i^{th} interface element, respectively, they can be calculated by Eq. (12) and Eq. (13) according to the stress state of the element; u_i is the mobilized shear displacement of the i^{th} interface element, u_{ip} is peak relative shear displacement of the i^{th} interface element.

2.4 The Factor of Safety Considering Interface Strain-softening Behavior

After getting the mobilized shear strength of any element of the interface, the shear resistance force of the i^{th} interface element can be calculated based on the element length falling within the three stages. This is achieved by calculating shear strength of the i^{th} interface element using the peak and residual friction angles

and adhesion intercepts, and multiplying the length of the i^{th} interface element with those conditions. Then the total resistance force can be obtained by summing the shear resistance force of all elements of the interface.

The shear resistance force of interface on the slope can be calculated by the following equation:

$$T_A = \sum T_{Ai} = \frac{\sum f(\sigma_{ni}, u_i)}{F' \cdot S} = \frac{\sum (l_{ip} \cdot \tau_{ip} + l_{ir} \cdot \tau_{ir})}{F' \cdot S} \quad (18)$$

where T_A is defined as the same as Eq. (6); T_{Ai} is shear resistance force of i^{th} interface element on the slope; l_{ip} is length of the i^{th} interface element of which the stresses condition fall within pre-peak state on the slope; l_{ir} is length of the i^{th} interface element of which the stresses condition fall within softening and residual states on the slope.

The shear resistance force of interface at the base can be calculated by the following equation:

$$T_p = \sum T_{pi} = \frac{\sum f(\sigma_{ni}, u_i)}{F' \cdot S} = \frac{\sum (s_{ip} \cdot \tau_p + s_{ir} \cdot \tau_r)}{F' \cdot S} \quad (19)$$

where T_p is defined as the same as Eq. (7); T_{pi} is shear resistance force of i^{th} interface element at the base; s_{ip} is length of the i^{th} interface element of which the stresses condition fall within pre-peak state at the base; s_{ir} is length of the i^{th} interface element of which the stresses condition fall within softening and residual states at the base.

By solving Eqs. (1)~(3), (5), (18) and (19), the factor of safety of the geomembrane barrier considering the interface strain softening property can be calculated with following equation:

$$F' \cdot S = \frac{\tan\left(\frac{\alpha + \omega}{2}\right) \cdot \sum (s_{ip} \cdot \tau_p + s_{ir} \cdot \tau_r) + \sin \alpha \cdot \sum (l_{ip} \cdot \tau_{ip} + l_{ir} \cdot \tau_{ir})}{W_A \cdot \sin \alpha^2} \quad (20)$$

3. Numerical Implementation of Nonlinear Strain Interface Softening Model

Due to its distinct advantages of solving large strain geotechnical problems, Fast Lagrange Analysis of Continua in Three Dimensions (FLAC^{3D}) has been widely used in numerical analysis of barrier systems of embankment and landfill (Wu *et al.*, 2008; Fowmes *et al.*, 2008). In order to get the distribution of mobilized shear stresses and displacements along the interface, the nonlinear strain softening interface model described in 2.2 is incorporated into FLAC^{3D} to analyze the geomembrane barrier systems of earth dam.

3.1 Improvement of the Interface Element in FLAC^{3D}

FLAC^{3D} provides interfaces that are characterized by Coulomb sliding and/or tensile and shear bonding. Interfaces have the properties of friction, cohesion, dilation, normal and shear stiffness, tensile and shear bond strength (Itasca Consulting Group, Inc., 2005). The interface element in FLAC^{3D} can only simulate the

interaction of which the relationship between shearing stress and displacement accord with perfect elasto-plastic model. But it cannot be used to simulate geosynthetic-soil interfaces which are characterized by the nonlinear and softening behaviors. So the interface element in FLAC^{3D} must be improved through imbedding a nonlinear strain softening interface model by user-defined fish program. The general methods of implementation are described as follows.

At every calculation step, the program first reads the normal effective stresses, shear stresses and shear displacements of every interface element. The state of every interface element is judged by the yield criterion according to the shear stresses and shear displacements. According to the state of the interface element, constitutive relations of corresponding stage are selected to calculate the relevant stiffness and strength parameters of the nonlinear strain softening interface mode. Then the calculated parameters are inputted to the interface element to carry out the calculation of next step. In this way, the program continuously circulates until all elements reach an equilibrium state. Due to the limit of length for this paper, the source code of the program cannot be presented in detail.

3.2 Validation of Improved Interface Model

In order to verify the effectiveness of the imbedded interface model, a simple numerical example is chosen to model the interface direct shear tests between a geomembrane and a geotextile. As shown in Fig. 4, the numerical model of the test is composed of two parts. The upper part is a shear box with soil in it, the lower one is a soil block where the geomembrane is glued at the top. The geotextile is fixed on the bottom surface of the upper box. In order to keep a constant contact area during shearing, the surface of the lower box is larger than that of the upper one. The imbedded nonlinear strain softening model is used to simulate the geomembrane-geotextile interface.

In order to compare the computational results with theoretical results, a linear elastic model was employed for the soil in the upper as well as the lower boxes. Gravity forces were not considered during the numerical exercise. Parameters of the nonlinear strain softening interface model are determined from the results of interface direct shear tests conducted by Anubhav (2010). The

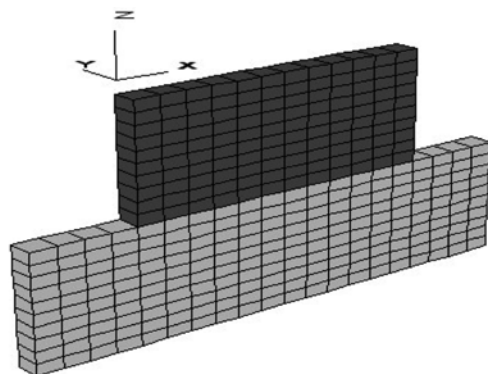


Fig. 4. Grids of Numerical Test Model

Table 1. Parameters for Displacement Softening Model of Interface

K	R_f	n	A	z	c_p (kPa)	ϕ_p (°)	c_r (kPa)	ϕ_r (°)	K_n (kN/m)
1374	0.51	0.5	0.879	1.51	4	36.7	0	31.7	1×10^9

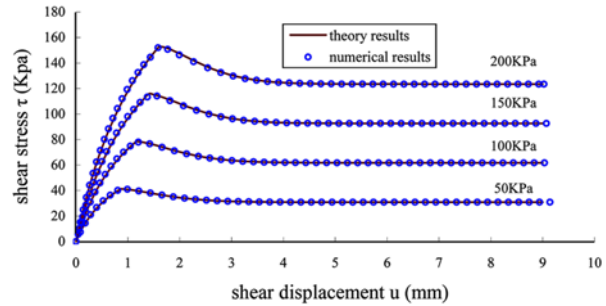


Fig. 5. Relationship Between Shear Stress and Displacement of Interface

parameters are listed in Table 1.

The relationships of averaged shear stress versus relative shear displacement of the interface under different normal pressures are shown in Fig. 5. It is seen that the numerical results show a good agreement with theory curves which were calculated by Eqs. (10)~(15) using the same parameters. The comparisons in Fig. 5 illustrate that the imbedded interface model in FLAC^{3D} is capable of modeling the nonlinear pre-peak behaviors as well as strain-softening post-peak response.

4. Examples Analysis

4.1 Numerical Model and Procedure

The finite difference code FLAC^{3D} is used to analyze the typical geomembrane surface barrier of earth dam. The barrier is a composite geomembrane consisting of a 0.8 mm thick HDPE geomembrane laminated to a 400 g/m² needle punched nonwoven geotextile at both sides. Their ultimate tensile strength (ASTM D4595) in machine direction and the cross-machine direction are 75.9 kN/m and 58.3 kN/m, respectively. The problem is simplified to two-dimensional model considering a slice of embankment with a thickness of 1m. The model is discretized by polyhedral elements. The finite difference grids of the model are shown in Fig. 6. The height of the earth dam is 60 m with slope of 1:2 at upstream and 1:1.6 at downstream. The slope where the geomembrane-soil interface located is 1:1.6. The Duncan E-B nonlinear elastic model (Clough and Duncan, 1970) is used for the

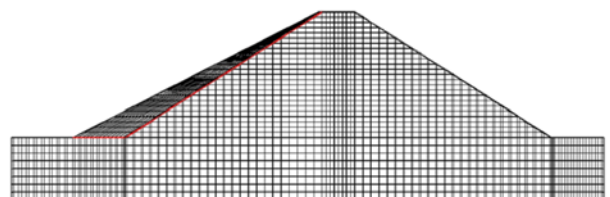


Fig. 6. Mesh of Calculation Model

Table 2. Parameters of Dam Model

Parameters	γ_d (kN/m ³)	C (kPa)	Φ (°)	K	n	R_f	K_b	m	K_{ur}	n_{ur}
Dam	21.0	0	35	550	0.45	0.80	220	0.5	1100	0.45
Foundation	21.0	0	32	500	0.48	0.82	200	0.4	1000	0.48
Protection cover	20.0	0	30.2	200	0.50	0.78	150	0.25	400	0.50

Table 3. Parameters for Geomembrane Interface

K	R_f	n	A	z	c_p (kPa)	ϕ_p (°)	c_r (kPa)	ϕ_r (°)	K_n (kN/m)
1853	0.53	0.51	0.89	1.43	3	32.1	0	28.3	1×10^9

soil of the dam and barrier. The nonlinear strain softening interface model incorporated into FLAC^{3D} is used to simulate the geomembrane-soil interface. The computational parameters for soils and nonlinear strain softening interface model are listed in Table 2 and 3, respectively. The parameters of soil an interface model are determined according to a project which is under design and research. In order to consider the effect of the construction procedure on the interface shear displacement, the process of numerical analysis is consistent with the construction procedure of the dam, namely, the fill process of dam is first simulated, and then the protection cover materials are filled over the geomembrane by 12 construction phases.

4.2 Results and Comparison

The stability of barrier was assessed by the method introduced above using the mobilized shear resistance from the results of numerical analysis. In order to compare with the results calculated by the developed method considering interface strain softening behavior, the LEM was also employed to calculate the factor of safety using three types of interface shear strength, namely, peak shear strength in the entire interface, residual shear strength in the entire interface, residual shear strength on the slope and peak shear strength at the base, respectively. The computational results of the different methods are listed in Table 4.

As is shown in Table 4, the factor of safety calculated by the method considering interface strain softening behavior is 1.30, which is less than 1.42 calculated by LEM using peak interface shear strength and larger than 1.22 calculated by LEM using residual interface shear strength. It is also can be found that the factor calculated by the method considering interface strain softening behavior is close to, and only slightly higher than 1.29 that calculated by LEM using residual shear strength on the slope and peak shear strength at the base.

4.3 Analysis and Discussion

The distribution of mobilized shear stresses, shear displace-

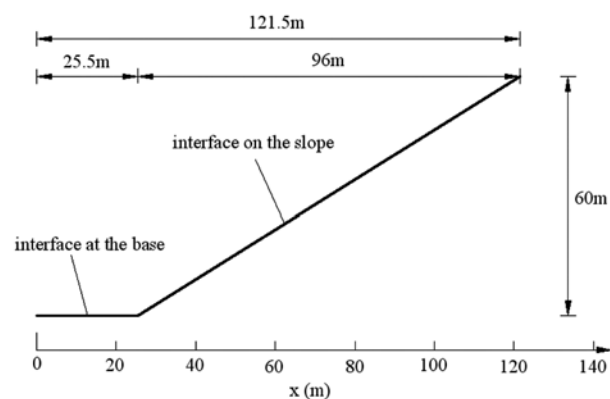


Fig. 7. Distance of Interface from the Toe of Dam

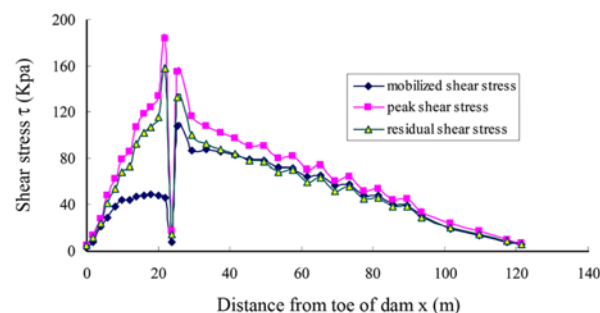


Fig. 8. Mobilized Shear Stress on Geomembrane Interface

ments and friction angles on the interface are plotted against the distance from the toe of dam. As is shown in Fig. 7, the interface of which the distance from toe of dam between 0 to 25.5 m represents the base of the protection cover, with the distance between 25.5 to 121.5 m being on the slope.

The distribution of mobilized shear stresses along the interface of the base and slope are shown in Fig. 8. The mobilized shear stresses increase with the reduction of elevation of the interface on the slope, reaching a peak near the toe of the slope. At the corner, the shear stresses decrease abruptly to about 2 Kpa. The reason that the maximum shear stress is not mobilized at the toe of the side slope may result from the geometry of the corner. Since the displacement of interface at the corner is restrained by the protection cover at the base. On the interface of the base, the mobilized shear stresses present a second peak in the middle, with lower values in two sides. The distribution of theoretical peak and residual shear strength along the interface are also presented in Fig. 8. They are calculated by Eqs. (12) and (13) using the normal effective stresses of every interface elements resulted from numerical analysis. It can be seen that the interface shear stresses in the middle of slope are mobilized with high degree. At

Table 4. Factors of Safety from Different Methods

Method considering interface strain softening behavior	Traditional LEM using different interface shear strength		
	Peak shear strength	Residual shear strength	Residual shear strength on the slope, Peak shear strength at the base
1.30	1.42	1.22	1.29

the base, the interface shear stresses are much lower than peak shear stresses. It shows a large deviation between mobilized shear stress and peak/residual shear stress at the base of dam. This is because that a smaller interface shear displacements (Fig. 9) have occurred in the part. Smaller interface shear displacements result in smaller mobilized interface shear stresses.

The distributions of actual shear displacements along the interface of the slope and base are shown in Fig. 9. In order to make comparison, theoretical peak shear displacements along the interface are also displayed in the Fig. 9. It is obvious that the interface shear displacements in the middle of the slope exceed the corresponding peak shear displacements. That indicates the interface stress condition in the middle of the slope fall into the softening and residual stage, in which the interface strain softening behaviors occurred. The shear displacements in other parts of the interface, especially at the base are much less than their peak shear displacements. That illustrates the interface stresses in this part remain in pre-peak stage.

The distribution of friction angles mobilized along the interface is shown in Fig. 10. The mobilized friction angles present a similar distribution form to that of shear stresses and displacements, with maximum interface friction angles which range between the peak and residual friction angles in the middle of the slope. It can be seen that the friction angles in this range are close to the residual friction angles. By comparing with shear displacements in Fig. 9, it may be resulted from the reduction of interface shear strength in the middle of the slope. It indicates again that the interface strain softening behaviors had occurred in most part of the slope.

4.4 Recommendation for Limit Equilibrium Analysis

It can be indicated from the analysis outlined above, the inter-

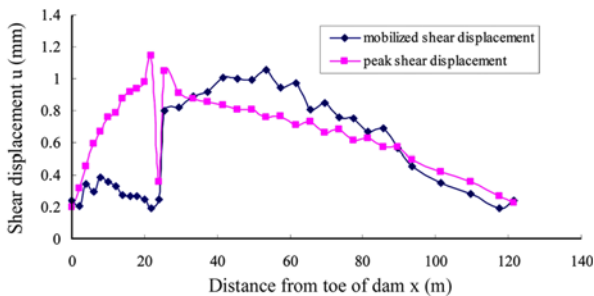


Fig. 9. Mobilized Shear Displacement on Geomembrane Interface

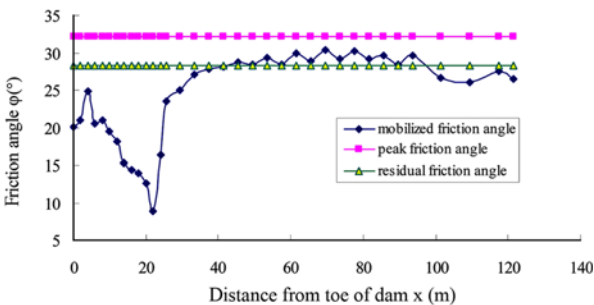


Fig. 10. Mobilized Shear Friction Angle on Geomembrane Interface

face stress condition at the base remain in the pre-peak stage, and the most part of the interface on the slope fall into the softening and residual stage. Through the previous analysis and comparison of the factors of safety calculated by different methods in Table 4, it can be suggested that the interface strain softening behavior reduce the shearing strength of interface in most part of the slope to values very close to the residual shearing strength. It is obviously non-conservative to perform limit equilibrium analyses using peak shear strengths. However, it is not necessary to assume complete strength reduction to residual strength along the entire interface. So a recommendation for assessment of the stability of geomembrane surface barrier of earth dam with limit equilibrium analysis can be proposed as following:

1. When calculate the shear resistance of interface on the slope with Eq. (6), the residual shear strength should be selected, namely, $\varphi = \varphi_r, c = c_r$;
2. When calculate the shear resistance of interface at the base with Eq. (7), the peak shear strength should be selected, namely, $\varphi = \varphi_p, c = c_p$.

5. Conclusions

A method which can consider strain softening behavior of geosynthetic interface was proposed to investigate the stability of the geomembrane surface barrier of earth dam. The formula of calculating the factor of safety was derived by combing the results of numerical analysis and the traditional LEM. The interface element of FLAC^{3D} was improved by to model the interface strain softening behavior in numerical analysis. An example of composite geomembrane lined earth dam was numerically analyzed with the developed method. The following conclusions can be drawn from the analysis:

1. The factor of safety of geomembrane surface barrier of earth dam calculated by the method considering interface strain softening behavior is very close to the result that calculated by LEM using residual shear strength on the slope and peak shear strength at the base. The result is lower than the one resulted from LEM using peak interface shear strength and higher than the one resulted from LEM using residual interface shear strength.
2. Due to the deformations of dam and barrier, large relative shear displacements occurred along the most part of interface on the slope, and small relative shear displacements occurred along the interface at the base. That indicates the most part of the interface on the slope fall into softening and residual stage, and the interface stress condition at the base are still in pre-peak stage.
3. It is unsafe to calculate the factor of safety using peak shear strength in LEM, and it is too conservative to use residual shear strength. It is suggested that using residual shear strength on the side slope and peak shear strength on the base is valid when assessing the stability of geomembrane surface barrier of earth dam with LEM.
4. Through analyzing the results from different methods, it can

be found the resistance of geomembrane surface barrier of earth dam is mainly provided by the mobilized shear stresses along failure plane. The factor of safety is dependent not only on the interface shear strength, but also on the deformation of dam, relative shear displacement and the shear stress-strain relationship of interface.

Acknowledgements

The project is supported by National Natural Science Foundation of China (No. 51079047), Ministry of Water Resources' Special Funds for Scientific Research on Public Causes (No. 201201039). Authors would like to thank the anonymous referees whose comments helped us improve the presentation of this paper.

References

- Anubhav, P. K. B. (2010). "Modeling of soil-woven geotextile interface behavior from direct shear test results." *Geotextiles and Geomembranes*, Vol. 28, No. 3, pp. 403-408.
- Byrne, R. J. (1994). "Design issues with strain-softening interfaces in landfill liners." *Proc. Waste Tech '94, Charleston*, South Carolina, USA, Session 4, Paper 4.
- Dixon, N., Blumel, W., Stoewahse, C., Kamusgisha, P., and Jones, D. R. V. (2002). "Geosynthetic interface shear behavior. Part 2: Characteristic values for use in design." *Ground Engineering*, Vol. 35, No. 3, pp. 49-53.
- Dixon, N., Jones, D. R. V., and Fowmes, G. J. (2006). "Interface shear strength and its use in reliability-based landfill stability analysis." *Geosynthetics International*, Vol. 13, No. 1, pp. 1-14.
- Duncan, J. M. and Chan, C. Y. (1970). "Nonlinear analysis of stress and strain in soils." *Journal of Soil Mechanics and Foundations Division*, ASCE, Vol. 96, No. 5, pp. 1629-1653.
- Jones, D. R. V. and Dixon, N. (1998). "Shear strength properties of geomembrane-geotextile interfaces." *Geotextiles and Geomembranes*, Vol. 16, No. 4, pp. 45-71.
- Jones, D. R. V. and Dixon, N. (2005). "Landfill lining stability and integrity - The role of waste settlement." *Geotextiles and Geomembranes*, Vol. 23, No. 1, pp. 27-53.
- Esterhuizen, J. J. B., Fliz, G. M., and Duncan, J. M. (2001). "Constitutive behavior of geosynthetic interface." *Journal of Geotechnical and Geoenvironmental Engineering*, ASCE, Vol. 127, No. 10, pp. 834-840.
- Filiz, G. M., Esterhuizen, J. J. B., Duncan, J. M. (2001). "Progressive failure of lined waste impoundments." *Journal of Geotechnical and Geoenvironmental Engineering*, ACSE, Vol. 127, No. 10, pp. 841-848.
- Fowmes, G. J., Dixon, N., and Jones, D. R. V. (2008). "Validation of a numerical modelling technique for multilayered geosynthetic landfill lining systems." *Geotextiles and Geomembranes*, Vol. 26, No. 2, pp. 109-121.
- Girard, H., Fisher, S., and Alonso, E. (1990). "Problems of friction posed by the use of geomembranes on dam slopes-examples and measurements." *Geotextiles and Geomembranes*, Vol. 9, No. 2, pp. 129-143.
- Giroud, J. P. and Beech, J. F. (1989). "Stability of soil layers on geosynthetic lining systems." *Proc. Geosynthetics '89*, San Diego, USA, pp. 35-46.
- Gomez, J. E. and Filz, G. M. (1999). "Influence of consolidation on the strength of the interface between a clay liner and a smooth geomembrane." *Proc., Geosynthetics 99*, Industrial Fabrics Association, Roseville, Minn., pp. 681-696.
- Itasca Consulting Group, Inc. (2005). *FLAC^{3D} (Fast Lagrangian analysis of continua in 3 dimensions) user manual*, Version 3.0, Minneapolis, USA.
- Koerner, R. M. and Hwu, B. L. (1991). "Stability and tension considerations regarding cover soils on geomembrane lined slopes." *Geotextiles and Geomembranes*, Vol.10, No. 4, pp. 335-355.
- Koerner, R. M. (1994). *Designing with geosynthetics*, 3rd Ed., Prentice-Hall, Englewood Cliffs, NJ.
- Liu, F. and Cheng, X. (2008). "Optimization and analysis of computational method for accessing the stability of geomembrane barrier of embankment." *Rock and Soil Mechanics*, Vol. 29, Supp., pp. 207-210 (in Chinese).
- Long, J. H., Gilbert, R. B., and Daly, J. J. (1994). "Geosynthetics loads in landfill slopes: Displacement compatibility." *Journal of Geotechnical Engineering*, ASCE, Vol. 120, No. 11, pp. 2009-2025.
- Ministry of Water Resources of the People's Republic of China (1998). *Standard for applications of geosynthetics in hydraulic and hydro-power engineering (SL/T225-98)*, China Water Power Press, Beijing (in Chinese).
- Seed, R. B., Mitchell, J. K., and Seed, H. B. (1988). *Slope stability failure investigation: Landfill unit B-19, phase I-A, Kettleman Hills, California*, Rep. No. UCB/GT/88-01, University of California, Berkeley, Calif.
- Seo, M. W., Park, I. J., and Park, J. B. (2004). "Development of displacement softening model for interface shear behavior between geosynthetics." *Soils and Foundations*, Vol. 44, No. 6, pp. 27-38.
- Shallenberger, W. C. and Filz, G. M. (1996). "Interface strength determination using a large displacement shear box." *Proc., 2nd Int. Congr. on Envir. Geotechnics*, Osaka, Japan, 1, pp. 147-152.
- Sia, A. H. I. and Dixon, N. (2007). "Distribution and variability of interface shear strength and derived parameters." *Geotextiles and Geomembranes*, Vol. 25, No. 3, pp. 139-154.
- Skempton, A. W. (1964). "Long term stability of clay slopes." *Geotechnique*, Vol.14, No. 2, pp. 77-101.
- Villard, P., Gourc, J. P., and Feki, N. (1999). "Analysis of Geosynthetic Lining Systems (GLS) undergoing large deformations." *Geotextiles and Geomembranes*, Vol. 17, No. 1, pp. 17-32.
- Wu, W., Wang, X. T., and Aschauer, F. (2008). "Investigation on failure of a geosynthetic lined reservoir." *Geotextiles and Geomembranes*, Vol. 26, No. 4, pp. 363-370.